

DMD #20115

**The mibefradil derivative NNC55-0396, a specific T-type calcium channel antagonist, exhibits less CYP3A4 inhibition than mibefradil**

Peter H. Bui, Arnulfo Quesada, Adrian Handforth, and Oliver Hankinson

Molecular Toxicology Interdepartmental Program, University of California, Los Angeles (UCLA)(P.B., O.H.), Department of Pathology and Laboratory Medicine, UCLA (P.B., O.H.), Jonsson Comprehensive Cancer Center, UCLA (P.B.,O.H.), Department of Neurobiology, UCLA(A.Q.), Neurology and Research Services, Veterans Affairs Greater Los Angeles(A.Q., A.H.).

DMD #20115

Running title: P450 inhibition comparison of NNC55-0396 and mibefradil

To whom correspondence should be addressed:

Oliver Hankinson, Ph.D.

Departmental of Pathology and Laboratory Medicine, David Geffen School of Medicine,  
University of California at Los Angeles.

650 Charles Young Drive, Los Angeles, CA. 90095

Tel: 310-825-2936 Fax: 310-794-9272 Email: [ohank@mednet.ucla.edu](mailto:ohank@mednet.ucla.edu)

Text: 40 pages

Table: 0

Figure: 7 Figures

Reference: 40 references

Abstract: 249 words

Introduction: 798 words

Discussion: 1537 words

Abbreviations: 6-OH-T, 6 $\beta$ -hydroxytestosterone; AHMC, 3-[2-N,N-diethyl-N-methylamino]-7-hydroxy-4-methylcoumarin; AMMC, 3-[2-N,N-diethyl-N-methylamino]-7-methoxy-4-methylcoumarin; BFC, 7-benzyloxy-4-trifluoromethylcoumarin; CYP, cytochrome P450; FU, fluorescence unit; HFC, 7-hydroxy-4-trifluoromethylcoumarin; HPLC, high-performance liquid chromatography; IC<sub>50</sub>, the half maximal inhibitory concentration; MFC, 7-methoxy-4-

DMD #20115

trifluoromethylcoumarin; P450, cytochrome P450; UGTs, uridine 5'-diphosphate-glucuronosyltransferases

DMD #20115

## Abstract

A novel mibefradil derivative, NNC55-0396, designed to be hydrolysis resistant was shown to be a selective T-type  $\text{Ca}^{2+}$  channel inhibitor without L-type  $\text{Ca}^{2+}$  channel efficacy. However, its effects on cytochrome P450s have not previously been examined. We investigated the inhibitory effects of NNC55-0396 toward 7 major recombinant human cytochrome P450s: CYP3A4, 2D6, 1A2, 2C9, 2C8, C19, and 2E1, and compared its effects with those of mibefradil and its hydrolyzed metabolite, Ro40-5966. Our results show that CYP3A4 and 2D6 are the two P450s most affected by mibefradil, Ro40-5966, and NNC55-0396. Mibefradil ( $\text{IC}_{50}=33\pm 3$  nM,  $\text{K}_i=23\pm 0.5$  nM) and Ro40-5966 ( $\text{IC}_{50}=30\pm 7.8$  nM,  $\text{K}_i=21\pm 2.8$  nM) have a nine to ten-fold greater inhibitory activity towards recombinant CYP3A4 benzyloxy-4-trifluoromethylcoumarin O-debenzylation activity than NNC55-0396 ( $\text{IC}_{50}=300\pm 30$  nM,  $\text{K}_i=210\pm 6$  nM). More dramatically, mibefradil ( $\text{IC}_{50}=566\pm 71$  nM,  $\text{K}_i=202\pm 39$  nM) shows 19-fold higher inhibition of CYP3A-associated testosterone  $6\beta$ -hydroxylase activity in human liver microsomes compared to NNC55-0396 ( $\text{IC}_{50}=11\pm 1.1$   $\mu\text{M}$ ,  $\text{K}_i=3.9\pm 0.4$   $\mu\text{M}$ ). Loss of testosterone  $6\beta$ -hydroxylase activity by recombinant CYP3A4 was shown to be time- and concentration-dependent with both compounds. However, NNC55-0396 ( $\text{K}_I=3.87\mu\text{M}$ ,  $\text{K}_{\text{inact}}=0.061$   $\text{min}^{-1}$ ) is a much less potent mechanism-based inhibitor than mibefradil ( $\text{K}_I=83$  nM,  $\text{K}_{\text{inact}}=0.048$   $\text{min}^{-1}$ ). In contrast, NNC55-0396 ( $\text{IC}_{50}=29\pm 1.2$  nM,  $\text{K}_i=2.8\pm 0.3$  nM) and Ro40-5966 ( $\text{IC}_{50}=46\pm 11$  nM,  $\text{K}_i=4.5\pm 0.02$  nM) have a three to four-fold greater inhibitory activity towards recombinant CYP2D6 than mibefradil ( $\text{IC}_{50}=129\pm 21$  nM,  $\text{K}_i=12.7\pm 0.9$  nM). Our results suggest that NNC55-0396 could be a more favorable T-

DMD #20115

type Ca<sup>2+</sup> antagonist than its parent compound, mibefradil, which was withdrawn from the market due to strong inhibition of CYP3A4.

DMD #20115

## Introduction

Voltage-gated  $\text{Ca}^{2+}$  channels are trans-membrane proteins involved in the regulation of cellular excitability and intracellular  $\text{Ca}^{2+}$  signaling (Huang et al., 2004). They are divided into two main types: the high-voltage-activated channels (L-, N-, P/Q-, and R-types), and the low-voltage-activated or T-type channels (Armstrong and Matteson, 1985; Perez-Reyes et al., 1998). Over the past three decades  $\text{Ca}^{2+}$  channel antagonists belonging to many structurally diverse classes, such as dihydropyridines, phenylalkylamines and benzothazepines, have been developed for the treatment of hypertension and chronic stable angina pectoris (Oparil and Calhoun, 1991). Their mode of action is to inhibit the inward current of  $\text{Ca}^{2+}$  through the slow L-type  $\text{Ca}^{2+}$  channels (Triggle, 1991). Mibefradil was reported in 1989 as a novel  $\text{Ca}^{2+}$  antagonist whose structure belongs to a new class, containing a tetraline ring linked to a benzimidazole group via an aliphatic tertiary amine (Figure 1) (Clozel et al., 1989). Mibefradil induces coronary and peripheral vasodilation through a direct effect on smooth muscle via blockade of T-type and L-type  $\text{Ca}^{2+}$  channels (Massie, 1997). Although mibefradil binds to a unique receptor site that overlaps with that of verapamil (Rutledge and Triggle, 1995), it does not depress myocardial contractility (Clozel et al., 1990), and it is not associated with negative inotropism (Portegies et al., 1991), which represents a therapeutic advantage for mibefradil.

Mibefradil was marketed by Roche as Posicor® after FDA approval in June 1997 for hypertension and chronic stable angina pectoris. About 200,000 American patients, and double that number worldwide, took the drug (SoRelle, 1998). Soon after its release, a

DMD #20115

number of case reports demonstrated the dangers of mibefradil drug interactions, including rhabdomyolysis and renal failure with simvastatin (Schmassmann-Suhijar et al., 1998), and symptomatic bradycardia with  $\beta$ -blockers (Rogers and Prpic, 1998). Mibefradil is a strong inhibitor of CYP3A4, 2D6 and P-glycoprotein (Ernst and Kelly, 1998; Wandel et al., 2000). It irreversibly inhibits CYP3A4 (Prueksaritanont et al., 1999), which is a serious problem as this P450 is responsible for the metabolism of more drugs than any other P450. Co-administration of mibefradil with terfenadine, cyclosporine A, or quinidine, for example, results in significant increases in their plasma concentrations; co-administration also leads to serious adverse effects with other drugs, including verapamil and diltiazem (Ernst and Kelly, 1998; Prueksaritanont et al., 1999; Varis et al., 2000). Since these drugs are all substrates for CYP3A4, it appears that inhibition of drug metabolism by mibefradil was the main cause for the adverse effects that led to the drug being withdrawn in June 1998 (Russell H. Ellison, 1997; SoRelle, 1998).

Mibefradil is metabolized mainly in the liver, producing as many as 30 metabolites (Wiltshire et al., 1997a; Wiltshire et al., 1997b). Metabolism consists of a combination of cytochrome P450-mediated oxidation, hydrolysis of the ester side-chain by CYP3A4 and esterases, and conjugation with glucuronic acid by uridine 5'-diphosphate-glucuronosyltransferases (UGTs) (Wiltshire et al., 1997b; Ernst and Kelly, 1998). One of the major hydrolyzed metabolites, Ro 40-5966 (Figure 1), was shown to strongly bind to L-type  $\text{Ca}^{2+}$  channels (Wu et al., 2000). L-type activity is thus a nonspecific feature of mibefradil administration (Li et al., 2005) and may account for other adverse effects associated with mibefradil. Recently, several analogs of mibefradil have been synthesized

DMD #20115

and tested for effects against T-type and L-type  $\text{Ca}^{2+}$  channels (Huang et al., 2004; Li et al., 2005). These analogs were designed to achieve more selectivity toward T-type  $\text{Ca}^{2+}$  channels. One of these is NNC55-0396, which has been shown to be equipotent as mibefradil in antagonizing the T-type  $\text{Ca}^{2+}$  channel, while exhibiting no L-type  $\text{Ca}^{2+}$  channel inhibition. NNC55-0396 was developed to be resistant to hydrolysis, by substituting the methoxyacetyl side chain of mibefradil with cyclopropanecarboxylate (Figure 1) (Huang et al., 2004; Li et al., 2005). This compound is not able to generate the hydrolyzed L-type  $\text{Ca}^{2+}$  channel blocker metabolite, Ro 40-5966, thus rendering NNC55-0396 selective to T-type  $\text{Ca}^{2+}$  channels (Huang et al., 2004; Li et al., 2005). Such a selective T-type  $\text{Ca}^{2+}$  channel antagonist, if found to possess a favorable safety profile, would represent a desirable therapeutic for chronic hypertension (Li et al., 2005), a disorder characterized by T-type  $\text{Ca}^{2+}$  channels upregulation in animals (Nuss and Houser, 1993).

A critical safety issue is whether NNC55-0396 has a more favorable P450 inhibition profile than mibefradil, since such information would predict its potential for drug interactions. After preliminary observations indicated differences in behavioral drug interactions involving mibefradil and NNC55-0396 in mice (our unpublished data), we conjectured that NNC55-0396 may have, despite similarities in structure, a more benign P450 inhibition profile than mibefradil. In this paper, we compared NNC55-0396's CYP450 inhibition profile to that of mibefradil and to that of the latter's hydrolyzed metabolite, Ro 40-5966, using both recombinant human P450s and human liver

DMD #20115

microsomes. These *in vitro* studies suggest that NNC55-0396 may be a more beneficial therapeutic agent for T-type Ca<sup>2+</sup> channels antagonist.

DMD #20115

## Materials and methods

### Chemical and Enzymes.

Bacterial membranes containing P450s and NADPH-P450-reductase (CPR), and human liver microsomes were obtained from BD Gentest (Franklin Lakes, NJ). Crude bacterial lysate containing the recombinant human CYP3A4 + CPR and P450 reaction buffer mixtures containing the NADP(+)/H regeneration enzymes were obtained from Biocatalytics, Inc (Pasadena, CA). Porcine liver esterase was obtained from Sigma-Aldrich (St. Louis, MO). The fluorescent substrates 3-[2-N,N-diethyl-N-methylamino]-7-methoxy-4-methylcoumarin (AMMC), 7-benzyloxy-4-trifluoromethylcoumarin (BFC), 7-methoxy-4-trifluoromethylcoumarin (MFC), and 7-hydroxy-4-trifluoromethylcoumarin (HFC) were purchased from BD Gentest (Franklin Lakes, NJ). Testosterone, 6- $\beta$ -hydroxy testosterone, harmaline, harmalol, mibefradil and NNC55-0396 were obtained from Sigma-Aldrich (St. Louis, MO). All the HPLC solvents (HPLC grade) were obtained from Sigma Aldrich (St. Louis, MO).

### $K_m$ determination for probe substrates

To determine the  $K_m$  of BFC and AMMC for recombinant CYP3A4 and 2D6 respectively, 7 different concentrations of substrates were incubated in 200  $\mu$ l reactions with 30 nM of recombinant P450 + CPR and 1x reaction buffer. The reactions were terminated after 10 minutes at 37°C by the addition of 200  $\mu$ l of ice-cold acetonitrile. A similar procedure was used to determine the  $K_m$  of testosterone and harmaline for human liver microsomes with the final concentration of microsomes being 0.13 mg/ml and time of incubation being 5 minutes at 37°C. All samples were analyzed in duplicate. The

DMD #20115

reactions were frozen in dry-ice methanol for 5 minutes to precipitate proteins, followed by centrifugation at 13,000 x g for 15 minutes to remove proteins. The supernatants were analyzed by HPLC with diode array and fluorescence detectors. The  $K_m$  of each substrate was then calculated by the Prism software using non-linear regression with the Michaelis-Menten equation.

### **Incubations of bacterially recombinant human P450s with substrates and inhibitors.**

Assays were conducted in 1.5 ml Eppendorf tubes in duplicate. 200  $\mu$ l reactions contained 1x reaction buffer mixture (pH 7.5, NADPH /NADP+ regenerating enzymes), 30 nM of recombinant P450 + CPR, 100  $\mu$ M of BFC or MFC, or 10  $\mu$ M of AMMC, and various concentrations of inhibitors. 100  $\mu$ M MFC was used as a probe substrate for CYP1A2, 2C9, 2C19, 2C8 and 2E1; 100  $\mu$ M BFC was used for CYP3A4, and 10  $\mu$ M AMMC was used for CYP2D6. The substrates and the inhibitors (mibefadil, Ro 40-5966, and NNC55-0396) were all dissolved in acetonitrile. 105  $\mu$ l of an enzyme buffer (EB) was prepared first which contained the 2x reaction buffer and 60 nM P450 enzymes. The EB was pre-warmed for 3 minutes at 37°C. The reaction was initiated by the addition of 95  $\mu$ l of substrate and inhibitor (S/I) mixture containing substrate and the inhibitor or vehicle (acetonitrile). 100 nM (low concentration) and 10  $\mu$ M (high concentration) inhibitors were used in the preliminary inhibition studies. 10  $\mu$ M of the inhibitors and eight successive 3:1 dilution concentrations were used in  $IC_{50}$  value determinations. The reactions were terminated after 20 minutes at 37°C by the addition of 200  $\mu$ l of ice-cold acetonitrile. The reactions were frozen in dry-ice methanol for 5 minutes to precipitate

DMD #20115

proteins, followed by centrifugation at 13,000 x g for 15 minutes to remove proteins. The supernatants were analyzed by HPLC with diode array and fluorescence detectors.

### **Incubations of human liver microsomes with testosterone, harmaline and inhibitors**

Incubations were conducted in duplicate with a 200  $\mu$ l volume in Eppendorf tubes. An enzyme buffer (EB) was prepared which contained 0.13 mg/ml of human liver microsomes and 2x reaction mixture buffer (pH 7.5, NADPH and NADP<sup>+</sup>/H regenerating enzymes and proprietary stabilizers, purchased from Biocatalytics, Inc). 105  $\mu$ l EB was pre-warmed for 3 minutes at 37°C. The reaction was initiated by adding 95  $\mu$ l of S/I mixture containing 200  $\mu$ M testosterone or 20  $\mu$ M harmaline and various concentration of inhibitors. 10  $\mu$ M of the inhibitors and eight successive 3:1 dilution concentrations were used in IC<sub>50</sub> value determinations. Acetonitrile was used as vehicle. The reactions were stopped after 5 minutes incubation at 37°C with 200  $\mu$ l of acetonitrile (2% acetic acid). The samples were frozen in dry-ice methanol for 5 minutes, followed by centrifugation at 13,000 x g for 15 minutes to remove proteins. The supernatant was analyzed by HPLC with diode array and fluorescence detectors.

### **Hydrolysis of mibefradil and NNC55-0396 using pig liver esterase and alkaline hydrolysis.**

40  $\mu$ M NNC55-0396 or mibefradil was incubated with 27 unit/ml of pig liver esterase for 1 hour at 37°C. The reactions were stopped with 1x volume acetonitrile and the incubation mixtures centrifuged at 13,000 x g for 20 minutes. Supernatants were analyzed by HPLC. Ro 40-5966, was synthesized using alkaline hydrolysis as described previously

DMD #20115

with some modifications (Wu et al., 2000), as follows: 500  $\mu$ l of 4 mM mibefradil in acetonitrile was added to 125  $\mu$ l 10N NaOH; the mixture was incubated for 12 minutes in a boiling water bath, and then neutralized with 125  $\mu$ l 5M hydrochloric acid. Due to the evaporation of acetonitrile, the volume was adjusted with acetonitrile to the starting volume of 500  $\mu$ l. Complete hydrolysis was checked by HPLC. All samples were analyzed with a C<sub>18</sub>-reverse phase column (Vydac, 150mm x 4.6mm, 5  $\mu$ ,). Mibefradil, NNC55-0396, and the Ro 40-5966 were monitored with fluorescence at 270 nm/300 nm (excitation  $\lambda$  /emission  $\lambda$ ) and with UV absorbance at 275 nm wavelength. The HPLC condition was set at 70% B isocratic for 30 minute (solvent A: H<sub>2</sub>O, 0.1% acetic acid, and 5 mM potassium phosphate, pH7.5; solvent B: acetonitrile).

### **Time- and concentration-dependent inhibition of recombinant CYP3A4 by NNC55-0396 and mibefradil**

Studies on the mechanism-based inhibition of CYP3A4 were performed using the testosterone 6- $\beta$ -hydroxylase assay at a high concentration of testosterone (500  $\mu$ M) in order to minimize the possibility of competitive inhibition by the inhibitors. Instead of bacterial membrane containing CYP3A4+CPR, crude bacterial lysate containing CYP3A4+CPR was used. The crude lysate was shown not to have more than 15 % auto-inactivation over the preincubation period in the absence of the inhibitors. All reactions were carried out at 37°C in duplicate. 100 nM of human recombinant CYP3A4+CPR was pre-incubated with NADPH (1 mM) in the presence of 0, 133, 400, 1200 and 3600 nM of NNC55-0396 or 44, 133, and 400 nM of mibefradil, in a final volume of 120  $\mu$ l containing 0.1 M potassium phosphate buffer (pH 7.5). At 0, 4, 8, 12, and 16 minutes, 20

DMD #20115

$\mu\text{l}$  aliquots of the reaction mixture were transferred into 180  $\mu\text{l}$  of secondary reactions containing 500  $\mu\text{M}$  of testosterone in the reaction buffer mixture (pH 7.5, NADPH and NADP<sup>+</sup>/H regenerating enzymes). CYP3A4 testosterone 6 $\beta$ -hydroxylase activity in the secondary reactions was then determined using HPLC. The kinetics of CYP3A4 inactivation were determined as follows: The initial rate constant for inactivation ( $K_{\text{obs}}$ ) at each concentration of inhibitor was estimated from the slope of the linear regression line (by Prism software) from the log of CYP3A4 remaining activity versus the preincubation time semi-log graph. Kinetic parameters ( $K_{\text{inact}}$  and  $K_{\text{I}}$ ) for the inactivation of CYP3A4 testosterone 6- $\beta$ -hydroxylase activity were then estimated from the reciprocal plot of the rate constant ( $K_{\text{obs}}$ ) versus the inhibitor concentrations.

### **Analytical Procedures**

All samples were analyzed using HPLC. The HPLC system consisted of the Shimadzu prominence series, including the LC-20 AT prominence LC pump, DGU-20A<sub>5</sub> degasser, CBM-20 prominence communications bus module, SPD-20A prominence UV/VIS detector, and RF-10AXL fluorescence detector (Shimadzu). A C<sub>18</sub> reversed-phase column (Water, 4.6 mm x 150 mm, 5  $\mu$ ) was used to detect and quantify metabolite products of MFC, BFC, and AMMC. The separation was achieved with 20% B from 0 to 5 minutes, linearly increased to 90% B from 5 minutes to 15 minutes, and was held until 20 minutes before returning to the starting condition (solvent A: 5 mM potassium phosphate, pH 7.5; solvent B: 100% acetonitrile; flow rate 1 ml/min). 7-hydroxy-4-trifluoromethylcoumarin (HFC), a product of MFC and BFC, and AHMC, a product of AMMC, were monitored by fluorescence detection with the setting at 410 nm/510 nm

DMD #20115

(excitation  $\lambda$  /emission  $\lambda$ ) and 390 nm/460 nm (excitation  $\lambda$  /emission  $\lambda$ ) respectively. For samples of testosterone and harmaline, a C<sub>18</sub> reversed-phase column (Dupont, 4.6 mm x 250 mm, 5  $\mu$ ) was used. The separation of testosterone samples was performed using 40% B from 0 to 5 minutes, increasing to 80% B from 5 minutes to 12 minutes, and then holding for another 17 minutes before returning to the starting condition (solvent A: H<sub>2</sub>O, 0.1% trifluoric acid; solvent B: 100% acetonitrile; flow rate 1ml/min). The testosterone metabolite, 6 $\beta$ -hydroxytestosterone, was monitored at a wavelength of 240 nm and eluted at 5.7 minutes. For harmaline, solvents were held isocratic at 30% B from 0 to 8 minutes. The gradient was linear from 30% B to 70% B from 8 to 12 minutes and held at 70% until 17 minutes; before returning to starting conditions (solvent A: H<sub>2</sub>O, 0.1% TFA; solvent B: 100% acetonitrile; flow rate 1ml/minutes). The harmaline metabolite, harmalol, was monitored with the fluorescence detector setting at 340 nm/495 nm (excitation  $\lambda$  /emission  $\lambda$ ), and eluted at 4.9 minutes.

### Data analysis

The P450s activities with and without inhibitors were measured by the area of products from the HPLC chromatograms. The activities of P450s in the presence of the inhibitors are addressed as the percentage activity of uninhibited P450s (area of product of the inhibited samples divided by the uninhibited samples times 100 percent). The IC<sub>50</sub> values were determined by Prism software, using the non-linear regression mode with one site competition. The equilibrium dissociation constant of inhibitor, K<sub>i</sub>, was calculated by Prism software using the IC<sub>50</sub> values, the given concentration and the K<sub>m</sub> of the respective probe substrate, and the equation,  $K_i = (IC_{50}) / (1 + [substrate] / K_m)$  (Linden, 1982).

DMD #20115

Calculations of the  $K_m$  for probe substrates and the kinetics of enzyme inactivations were described previously above. The t-test was used for statistical analysis (Prism software).

DMD #20115

## Results

### Comparison of NNC55-0396's P450 inhibition profile to that of mibefradil

Seven major recombinant human cytochrome P450s: CYP3A4, 1A2, 2E1, 2D6, 2C8, 2C19, and 2C9 were chosen for inhibition studies with mibefradil and NNC55-0396. It has been demonstrated that these P450s participate in the metabolism of approximately 80% of therapeutic drugs (Wienkers and Heath, 2005). To obtain a preliminary look at the P450 inhibitory profiles for mibefradil and NNC55-0396, two concentrations of the inhibitors were chosen, 100 nM and 10  $\mu$ M. These two concentrations represent the low and the high concentrations and cover the range of therapeutic plasma concentrations of the inhibitors, since it has been reported that the human therapeutic plasma concentration of mibefradil ranges from 300 ng/ml to 1000 ng/ml after doses of 50 mg/day to 100 mg/day, which correspond to 0.5  $\mu$ M to 1.8  $\mu$ M mibefradil (Wiltshire et al., 1997a; Welker and Banken, 1998). At 100 nM, mibefradil exhibited more than a 2-fold greater inhibition than NNC55-0396 for CYP3A4 (63% and 27%, respectively,  $p < 0.001$ , Figure 2F). At 10  $\mu$ M, both mibefradil and NNC55-0396 inhibited over 90% of CYP3A4 activity (Figure 2F). Mibefradil and NNC55-0396 had opposite inhibitory effects to those above for CYP2D6. At 100 nM, NNC55-0396 exhibited more than 2-fold greater inhibition of CYP2D6 compared to mibefradil (55% and 23%, respectively,  $p < 0.001$ , Figure 2G). At 10  $\mu$ M, both compounds inhibited CYP2D6 >95% (Figure 2G). Our mibefradil data are in agreement with previous reports demonstrating that mibefradil strongly inhibits CYP3A4 and 2D6 (Ernst and Kelly, 1998; Prueksaritanont et al., 1999; Stresser et al., 2000). Mibefradil at 100 nM slightly inhibited CYP2C9 (11 %;  $p < 0.05$ , Figure 2C), whereas NNC55-0396 at 100 nM failed to do so (Figure 2C). Neither

DMD #20115

CYP2C8 nor 2C19 was inhibited by 100 nM mibefradil or NNC55-0396, and 10  $\mu$ M concentrations of these compounds inhibited CYP2C9, CYP2C8 and CYP2C19 considerably less than they inhibited CYP3A4 and CYP2D6 (Figures 2C, 2D, and 2E). CYP2E1 and CYP1A2 were not inhibited by either compound, even at 10  $\mu$ M (Figure 2A and 2B).

### **IC<sub>50</sub> and K<sub>i</sub> values of mibefradil and NNC55-0396 for recombinant CYP3A4 and CYP2D6**

Our preliminary look at the P450 inhibitory profiles for mibefradil and NNC55-0396, therefore showed that of the above cytochrome P450s, only recombinant CYP3A4 and 2D6 exhibited marked inhibition by both compounds at low concentrations. We therefore went on to compare the inhibitory effects of the above compounds on CYP3A4 and CYP2D6 by estimating their IC<sub>50</sub> and K<sub>i</sub> values. We determined the IC<sub>50</sub> values of mibefradil and NNC55-0396 using eight inhibitor concentrations generated by serial 1:3 dilutions from 10  $\mu$ M. While the IC<sub>50</sub> value expresses the concentration of the inhibitor that competes for half the specific substrate binding sites, it does not quantify the affinity of the inhibitor for the enzyme. K<sub>i</sub>, the equilibrium dissociation constant, is a measure of this last parameter. It is the concentration of the inhibitor that will bind to half the binding sites at equilibrium, and is can calculated based on the IC<sub>50</sub> values of inhibitor, the substrate's K<sub>m</sub> and the given substrate concentration (Linden, 1982) The K<sub>m</sub> of BFC and AMMC, the substrates for CYP3A4 and 2D6, respectively, were determined to be 240  $\mu$ M and 1.08  $\mu$ M respectively. For CYP3A4 inhibition, the IC<sub>50</sub> and K<sub>i</sub> values of mibefradil were 33  $\pm$  3 nM and 23  $\pm$  0.5 nM, whereas the IC<sub>50</sub> and K<sub>i</sub> values of NNC55-

DMD #20115

0396 were  $300 \pm 30$  nM and  $210 \pm 6$ nM (Figure 3A), demonstrating that NNC55-0396 is nine times less inhibitory than mibefradil towards recombinant human CYP3A4 ( $p < 0.001$ , Figure 3A). Our mibefradil  $IC_{50}$  value for recombinant CYP3A4 is similar to that reported by Stresser et al. (Stresser *et al.*, 2000). For CYP2D6 inhibition, mibefradil had  $IC_{50}$  and  $K_i$  values of  $129 \pm 21$  nM and  $12.7 \pm 0.9$  nM while NNC55-0396 had  $IC_{50}$  and  $K_i$  values of  $29 \pm 1.2$  nM and  $2.8 \pm 0.3$  nM, representing a four-fold greater inhibition efficacy for NNC55-0396 compared to mibefradil ( $p < 0.005$ , Figure 3B).

### **The effects of mibefradil and NNC55-0396 on cytochrome P450 activities in human liver microsomes**

To further verify mibefradil's and NNC55-0396's inhibitory effects on human CYP3A4 and 2D6 we used human liver microsomes, (which contain CYP3A4, 2D6 and other P450s). CYP3A4 is the main hepatic enzyme involved in testosterone 6 $\beta$ -hydroxylation (Gillam et al., 1993), while CYP2D6 is the main hepatic enzyme responsible for harmaline metabolism (Yu et al., 2003). Thus, testosterone and harmaline were used as substrates to determine the activities of CYP3A4 and 2D6 in human liver microsomes. The  $K_m$  of testosterone and harmaline were determined to be 111  $\mu$ M and 74  $\mu$ M respectively. Eight concentrations of mibefradil and NNC55-0396 generated by serial 1:3 dilutions of 10  $\mu$ M were used to determine their  $IC_{50}$  and  $K_i$  values for CYP3A4 and 2D6 in liver microsomes. The present data demonstrates that mibefradil was 19 times more inhibitory than NNC55-0396 for testosterone 6 $\beta$ -hydroxylation in the human liver microsomes, because the former had  $IC_{50}$  and  $K_i$  values of  $566 \pm 71$  nM and  $202 \pm 39$  nM, respectively, while the latter had  $IC_{50}$  and  $K_i$  values of  $11.0 \pm 1.1$   $\mu$ M and  $3.9 \pm 0.4$

DMD #20115

$\mu\text{M}$  respectively ( $p < 0.001$ , Figure 4A). In contrast, the data demonstrated that NNC55-0396 was 15 times more inhibitory than mibefradil for harmaline metabolism in the human liver microsomes ( $p < 0.01$ , Figure 4B). NNC55-0396 had  $\text{IC}_{50}$  and  $\text{K}_i$  values of  $72.6 \pm 6 \text{ nM}$  and  $57.1 \pm 5 \text{ nM}$ , while mibefradil had  $\text{IC}_{50}$  and  $\text{K}_i$  values of  $1111 \pm 52 \text{ nM}$  and  $833 \pm 39 \text{ nM}$  for CYP2D6 in liver microsomes (Figure 4B).

### **Effects of esterase on mibefradil and NNC55-0396**

Mibefradil is easily hydrolyzed by enzymes after it enters the cell (Wiltshire et al., 1992; Wu et al., 2000). Its hydrolyzed metabolite, Ro 40-5966, has been shown to block L-type  $\text{Ca}^{2+}$  channels (Wu et al., 2000). NNC55-0396 has more specific inhibitory activity towards T-type  $\text{Ca}^{2+}$  channels than mibefradil (Huang et al., 2004; Li et al., 2005), most likely due to its resistance to hydrolysis conferred by the replacement of the methoxy acetate chain with cyclopropanecarboxylate. To test whether that NNC55-0396 is more resistant to hydrolysis by esterase than mibefradil, both were incubated with pig liver esterase. Pig liver esterases are commonly used for *in vitro* study since human esterases are not available. Our data shows that after one hour at  $37^\circ\text{C}$ , 10 % of mibefradil was hydrolyzed by esterase to yield a product peak at 15.5 minutes that corresponds to the Ro 40-5966 standard (Figure 5B), whereas no hydrolyzed product was detected in NNC55-0396 sample incubated with esterase (Figure 5A). Thus, mibefradil is susceptible to hydrolysis by the esterase yielding Ro 40-5966, whereas NNC55-0396 is not. However, whether or not NNC55-0396 is resistant to hydrolysis in the human needs to be examined.

DMD #20115

### **P450 inhibition profile of mibefradil's hydrolyzed metabolite, Ro 40-5966 in comparison to mibefradil and NNC55-0396.**

According to Wiltshire and coworkers, 20% to 32% of mibefradil is converted to Ro 40-5966 after clinical administration (Wiltshire et al., 1992; Wiltshire et al., 1997a).

Although it has been shown here and by others that mibefradil inhibits several P450s, it has not previously been investigated whether Ro 40-5966 can also inhibit P450s. We therefore tested Ro 40-5966's inhibition towards recombinant CYP2D6, 3A4, 2C9, 1A2, 2C19, and 2C8 (Figure 6A-F). As with mibefradil and NNC55-0396, only recombinant CYP3A4 and 2D6 showed strong inhibition by Ro 40-5966 (Figure 6A and 6B). Our results demonstrate that Ro 40-5966 has  $IC_{50}$  and  $K_i$  values of  $30 \pm 7.8$  nM and  $21 \pm 2.8$  nM for CYP3A4, which are comparable to mibefradil's values of  $33 \pm 3$  nM and  $23 \pm 0.5$  nM (Figure 6B and 3A). These  $IC_{50}$  and  $K_i$  values indicate that like mibefradil, Ro 40-5966 is 9 to 10 times more inhibitory than NNC55-0396 towards recombinant CYP3A4, which has  $IC_{50}$  and  $K_i$  values of  $300 \pm 30$  nM and  $210 \pm 6$  nM (Figure 3A). For recombinant CYP2D6, Ro 40-5966 was determined to have  $IC_{50}$  and  $K_i$  values of  $46 \pm 11$  nM and  $4.5 \pm 0.02$  nM (Figure 6A), which are comparable to the values for NNC55-0396 ( $IC_{50} = 29 \pm 1.2$  nM and  $K_i = 2.8 \pm 0.3$  nM, Figure 3B). Comparison of the inhibition values of Ro 40-5966 to that of mibefradil ( $IC_{50} = 129 \pm 21$  nM and  $K_i = 12.7 \pm 0.9$  nM, Figure 3B) indicates a three-fold greater inhibition efficacy of Ro 40-5966 toward CYP2D6 ( $p < 0.05$ , Figure 6A and 3B). Inhibition of 2C19, and 1A2 by Ro 40-5966 was observed only at the supra-optimal concentration of 10  $\mu$ M ( $p < 0.001$ , Figures 6D, and 6E). The  $IC_{50}$  for CYP2C9 was estimated to be  $823 \pm 390$  nM (Figure 6C). Whereas, there was no significant inhibition of CYP2C8 even at 10  $\mu$ M concentration (Figure 6F).

DMD #20115

## **Inhibition mechanism of mibefradil and NNC55-0396 towards recombinant**

### **CYP3A4**

Mibefradil has been shown to be a powerful mechanism-based inhibitor of CYP3A4 (Prueksaritanont et al., 1999). Our preliminary data indicated that NNC55-0396 also exhibited time-dependent inactivation of CYP3A4. To further investigate the inhibition mechanism of NNC55-0396, and to compare it with that of mibefradil, mechanism-based inhibition assays were performed using recombinant human CYP3A4-catalyzed testosterone 6 $\beta$  hydroxylase activity. Crude lysate containing CYP3A4 was used instead of a membrane fraction containing the enzyme, because the latter was shown to have a 50% decrease in activity during the period of incubation even in the absence of inhibitor, whereas the former showed no more than 15 % auto-inactivation. The kinetic parameters, such as the concentration required for half-maximal inactivation ( $K_I$ ), and the rate constant of maximal inactivation at saturation ( $K_{inact}$ ), were determined. These numbers were used to compare the inactivation efficiency of mibefradil and NNC55-0396 towards the CYP3A4 enzyme. Preincubation of recombinant CYP3A4 with various concentrations of mibefradil and NNC55-0396 in the presence of NADPH resulted in a time- and concentration-dependent loss of testosterone 6 $\beta$ -hydroxylase activity. However, NNC55-0396 significantly caused time-dependent inactivation of testosterone 6 $\beta$ -hydroxylase only at the high concentrations 1.2 and 3.6  $\mu$ M, compared to the control ( $p < 0.05$ , Figure 7C). The  $K_I$  and  $K_{inact}$  of NNC55-0396 for CYP3A4 were estimated to be 3.87  $\mu$ M and 0.061  $\text{min}^{-1}$ , respectively (Figure 7D).

DMD #20115

In contrast, mibefradil significantly caused time-dependent loss of testosterone 6 $\beta$ -hydroxylase activity even at 44 nM, the lowest concentration tested ( $p < 0.01$ , Figure 7A). The estimated  $K_I$  and  $K_{inact}$  of mibefradil were 83 nM and  $0.048 \text{ min}^{-1}$ , respectively (figure 7B). The  $K_I$  of mibefradil is therefore 47 times lower than that of NNC55-0396. From the kinetics values, the inactivation efficiency ( $E_{inact} = K_{inact}/[K_I + I]$ ) can be estimated (Zhou et al., 2005).  $E_{inact}$  of mibefradil is at least 3.3 fold higher than that of NNC55-0396 for inactivating CYP3A4 testosterone 6 $\beta$ -hydroxylase, when the inhibitor concentrations are at 1  $\mu\text{M}$  or less. The lower the inhibitors' concentrations are the greater will be the difference in inactivation efficiency between mibefradil and NNC55-0396.

DMD #20115

## Discussion

Mibefradil, a potent T-type  $\text{Ca}^{2+}$  channel inhibitor, was marketed clinically for cardiac indications, but was withdrawn after serious drug-drug interactions emerged, particularly due to CYP3A4 inhibition and inactivation. It also has the disadvantage of L-type  $\text{Ca}^{2+}$  channel antagonism contributed by its hydrolyzed metabolite, Ro 40-5966. Recently, a mibefradil derivative, NNC55-0396, designed to be hydrolysis resistant, was shown to be a selective T-type  $\text{Ca}^{2+}$  channel inhibitor without L-type  $\text{Ca}^{2+}$  channel efficacy (Li et al., 2005). Whether NNC55-0396 will deliver a clinical benefit with minimized drug-drug interactions is not known. However, potential adverse effects can often be predicted. In the preclinical drug discovery and development phase, studies of cytochrome P450 enzyme inhibition and inactivation have become one of the major approaches for the *in vitro* assessment of the risk associated with new molecular entities (NMEs) as precipitants of drug-drug interactions (Venkatakrisnan et al., 2007). Thus, this report is the first *in vitro* study of NNC55-0396's effects on human cytochrome P450s in which its effects are also being compared to mibefradil and its hydrolyzed metabolite, Ro 40-5966. The study will provide crucial information about the possible risk associated with NNC55-0396.

Using seven major recombinant human cytochrome P450s and human liver microsomes, and HPLC as a detection and analytical method, we demonstrated that compared to mibefradil, NNC55-0396 has a significant less inhibitory profile for the CYP3A4 activity of recombinant CYP3A4 as well as CYP3A4-dependent activity in human liver microsomes. The  $\text{IC}_{50}$  and  $\text{K}_i$  of NNC55-0396 are both 9 to 10 times higher than those of

DMD #20115

mibefradil for recombinant CYP3A4, suggesting that the former compound is 9 to 10 times less inhibitory than the latter. The differences in these values are more dramatic when inhibition of testosterone 6 $\beta$ -hydroxylase activity of CYP3A was examined in human liver microsomes. The IC<sub>50</sub> and K<sub>i</sub> of NNC55-0396 are 19-fold higher than that of mibefradil. The higher IC<sub>50</sub> and K<sub>i</sub> values observed for CYP3A4 in human liver microsomes compared with the values for recombinant CYP3A4 may result from the presence of other microsomal proteins that bind to the inhibitors, or to the presence of other enzymes that can metabolize the inhibitors, thus making them less available to inhibit the targeted enzyme (Wiltshire et al., 1997a). Moreover, the difference could have been contributed by different substrates being used.

Previous evidence suggested that mibefradil metabolites also inhibit CYP3A4 (Prueksaritanont et al., 1999; Ma et al., 2000), but the degree of inhibition has not previously been investigated. Mibefradil is hydrolyzed by esterase and by CYP3A4 to generate a hydroxyl mibefradil, Ro 40-5966 (Wiltshire et al., 1997a), one of many mibefradil metabolites shown to contribute to the L-type Ca<sup>2+</sup> channel non-specific inhibition of mibefradil (Wu et al., 2000). Our results demonstrate that Ro 40-5966 inhibits CYP3A4 with an efficacy comparable to mibefradil, and thus is 10 times more inhibitory than NNC55-0396. This result indicates that the Ro 40-5966 metabolite might also contribute to mibefradil's drug interactions.

When using a time and concentration dependent inhibition assay, we found that, NNC55-0396 also caused time dependent inactivation of CYP3A4, but was less potent in this

DMD #20115

regard than mibefradil. The concentration of NNC55-0396 required for half-maximal inactivation ( $K_I$ ) of CYP3A4 is 3.4  $\mu\text{M}$  which is 47-fold higher than that of mibefradil. Its  $t_{1/2\text{inact}}$  ( $0.693/K_{\text{inact}}$ ) is just slightly shorter (11.3 min) than that of mibefradil (14.4 min).  $K_I$  values can be used to classify inhibitory potency of compounds (Zhou et al., 2005). The  $K_I$  value of NNC55-0396 is comparable to the  $K_I$  values of verapamil (1.7  $\mu\text{M}$ ) and diltiazem (2.0  $\mu\text{M}$ ), which are the  $\text{Ca}^{2+}$  channels antagonists being used as antihypertensive drugs and are currently available on the market (Zhou et al., 2005). In addition, verapamil and diltiazem even have shorter  $t_{1/2\text{inact}}$  (7.70 and 6.30 minutes, respectively) (Zhou et al., 2005) than that of NNC55-0396.

CYP3A4 is responsible for metabolizing 50-60% of all therapeutic drugs that are metabolized by P450s in humans (Thummel et al., 1996). Drugs that inhibit CYP3A4 such as ketoconazole, cisapride, ritonavir, and nefazodone have been found to cause deleterious side effects when coadministered with other drugs. Many drugs that strongly inhibit CYP3A4 such as mibefradil have therefore been withdrawn from the market (Russell H. Ellison, 1997; SoRelle, 1998; Bohets et al., 2000; Watanabe et al., 2007). Mibefradil was shown to strongly inhibit CYP3A4 via mechanism-based inactivation at its relevant therapeutic concentration. Such inhibition is highly potent because it irreversibly reduces the amount of the enzyme available, so that restoration of activity requires the synthesis of new enzyme. The pharmacokinetics of NNC55-0396 needs to be determined in order to get an accurate assessment of its clinical drug-drug interaction outcomes. However, if the pharmacokinetics of NNC55-0396 are the same as mibefradil, then NNC55-0396 would likely be a lesser or even non-potent mechanism-based

DMD #20115

inhibitor of CYP3A4 *in vivo*. Given the total  $C_{\max}$  of mibefradil of around 0.5 to 1.8  $\mu\text{M}$  (Wiltshire et al., 1997a; Welker and Banken, 1998), and the fact that more than **90%** of mibefradil is protein-bound, the available plasma concentration of NNC55-0396 will be much below its apparent  $K_i$  (3.9  $\mu\text{M}$ ), and the  $C_{\max}/K_i$  ratio of NNC55-0396 would be less than 1 (based on the  $K_i$  derived from human liver microsomes). This ratio indicates that drug-drug interaction is unlikely, but possible, because according to the current FDA guidelines for predicting the likelihood of clinically relevant drug-drug interaction, if  $C_{\max}/K_i > 1$ , a drug interaction is likely, if  $C_{\max}/K_i > 0.1$ , a drug interaction is possible, and if  $C_{\max}/K_i < 0.1$ , a drug interaction is unlikely. It is however also possible that the NNC55-0396's  $C_{\max}$  will be higher in clinical settings. If this is the case, then the  $C_{\max}/K_i$  ratio may be higher than 1 and drug-drug interaction is likely.

CYP2D6 has been reported to be inhibited by mibefradil, but the  $\text{IC}_{50}$  and  $K_i$  values have not previously been determined. We are the first to report mibefradil's  $\text{IC}_{50}$  and  $K_i$  values for CYP2D6, and to demonstrate that Ro 40-5966 strongly inhibits CYP2D6 with relatively lower  $\text{IC}_{50}$  and  $K_i$  than its parent compound. This could have also contributed to the complexity of mibefradil's toxicity. Our results also demonstrate that NNC55-0396 inhibits CYP2D6 with relatively low  $\text{IC}_{50}$  and  $K_i$  values with both recombinant CYP2D6 and human liver microsomes. This strong inhibition of CYP2D6 could be a concern because CYP2D6, though playing a less important role than CYP3A4 in drug metabolism, is the second most significant P450 in this regard, since it metabolizes 20-25% of clinically used drugs (Ingelman-Sundberg, 2004). However, many strong

DMD #20115

inhibitors of CYP2D6 with low IC<sub>50</sub> values, such as terbinafine, dextromethorphan, quinidine, and propranolol are currently on the market.

Although, mibefradil, NNC55-0396 and Ro 40-5966 also inhibit CYP2C9, 2C8 and 2C19, they do so only at high concentrations (10 μM), indicating that relative high dosages of these drugs would need to be taken to reach sufficiently high plasma levels to inhibit these enzymes. In addition, CYP2C9, 2C8 and 2C19 have a less important role clinically than CYP3A4 in drug metabolism (Ingelman-Sundberg, 2004). However, they are not irrelevant in drug- drug interactions.

Clinically, T-type Ca<sup>2+</sup> channels have represented important therapeutic targets in various types of diseases, from cardiovascular diseases, diabetes, neurological diseases, to cancer (Li et al., 2005; Tanaka and Shigenobu, 2005; Panner and Wurster, 2006). Besides their strong association with cardiovascular disease, T-type Ca<sup>2+</sup> channels are associated with cancer cell proliferation, and inhibiting T-type Ca<sup>2+</sup> channels protects from delayed ischemia-induced damage (Nikonenko et al., 2005). T-type Ca<sup>2+</sup> channels are also implicated in the pathogenesis of epilepsy and neuropathic pain (Tanaka and Shigenobu, 2005). Thus far, highly selective T-type Ca<sup>2+</sup> channel antagonists have not been clinically available. Several candidate drugs that potently inhibit T-type Ca<sup>2+</sup> channels unfortunately, like mibefradil, also strongly inhibit L-type Ca<sup>2+</sup> channels. Interestingly, a methoxyacetyl group of mibefradil seems to play not only an important role in selectivity towards the Ca<sup>2+</sup> channels but also in P450 inhibition. We and others (Huang et al., 2004; Li et al., 2005) found changes in inhibition specificities when this ester group is

DMD #20115

modified. Thus, it is probable that additional non-hydrolysable analogs of mibefradil could be designed that exert less inhibition of CYP3A4 and CYP2D6 but still retain the same potency for T-type  $\text{Ca}^{2+}$  channel antagonism.

In summary, our data suggest that NNC55-0396 is a more favorable T-type  $\text{Ca}^{2+}$  channel antagonist than its parental compound, mibefradil, for the following reasons: (i) NNC55-0396 is a selective T-type  $\text{Ca}^{2+}$  channels blocker without L-type  $\text{Ca}^{2+}$  channel efficacy (Li *et al.*, 2005). (ii) It has a considerably weaker inhibitory profile for CYP3A4 than mibefradil. Such inhibition of CYP3A4 was an important problem that contributed to mibefradil's withdrawal from the market. (iii) Unlike mibefradil, NNC55-0396 is not hydrolyzed by esterase to form Ro 40-5966, itself a very potent CYP3A4 and L-type  $\text{Ca}^{2+}$  antagonist (Wu *et al.*, 2000). However, freedom from CYP3A4-based interactions will also depend on the pharmacokinetic properties of NNC55-0396. Predicting drug-drug interaction is even more challenging when it involves mechanism-based inactivation of enzyme, since the clinical outcomes depend on a number of factors, including the pharmacokinetic effects ( $K_i$ ,  $K_{\text{inact}}$ , and partition ratio), and the zero-order synthesis rate of new or replacement enzyme (Zhou *et al.*, 2005). Nevertheless, our findings are highly suggestive for a weaker interaction CYP3A4 profile for NNC55-0396. More work is needed, however, to establish whether its differences from mibefradil may be clinically meaningful.

DMD #20115

### **Acknowledgements**

Thanks are extended to Dr. Curt Eckhert for allowing us to use his HPLC equipment.

DMD #20115

## References

- Armstrong CM and Matteson DR (1985) Two distinct populations of calcium channels in a clonal line of pituitary cells. *Science* **227**:65-67.
- Bohets H, Lavrijsen K, Hendrickx J, van Houdt J, van Genechten V, Verboven P, Meuldermans W and Heykants J (2000) Identification of the cytochrome P450 enzymes involved in the metabolism of cisapride: in vitro studies of potential co-medication interactions. *Br J Pharmacol* **129**:1655-1667.
- Clozel JP, Banken L and Osterrieder W (1989) Effects of Ro 40-5967, a novel calcium antagonist, on myocardial function during ischemia induced by lowering coronary perfusion pressure in dogs: comparison with verapamil. *J Cardiovasc Pharmacol* **14**:713-721.
- Clozel JP, Veniant M and Osterrieder W (1990) The structurally novel Ca<sup>2+</sup> channel blocker Ro 40-5967, which binds to the [3H] desmethoxyverapamil receptor, is devoid of the negative inotropic effects of verapamil in normal and failing rat hearts. *Cardiovasc Drugs Ther* **4**:731-736.
- Ernst ME and Kelly MW (1998) Mibefradil, a pharmacologically distinct calcium antagonist. *Pharmacotherapy* **18**:463-485.
- Gillam EM, Baba T, Kim BR, Ohmori S and Guengerich FP (1993) Expression of modified human cytochrome P450 3A4 in *Escherichia coli* and purification and reconstitution of the enzyme. *Arch Biochem Biophys* **305**:123-131.
- Huang L, Keyser BM, Tagmose TM, Hansen JB, Taylor JT, Zhuang H, Zhang M, Ragsdale DS and Li M (2004) NNC 55-0396 [(1S,2S)-2-(2-(N-[(3-benzimidazol-2-yl)propyl]-N-methylamino)ethyl)-6-fluoro-1,2,3,4-tetrahydro-1-isopropyl-2-

DMD #20115

- naphtyl cyclopropanecarboxylate dihydrochloride]: a new selective inhibitor of T-type calcium channels. *J Pharmacol Exp Ther* **309**:193-199.
- Ingelman-Sundberg M (2004) Pharmacogenetics of cytochrome P450 and its applications in drug therapy: the past, present and future. *Trends Pharmacol Sci* **25**:193-200.
- Li M, Hansen JB, Huang L, Keyser BM and Taylor JT (2005) Towards selective antagonists of T-type calcium channels: design, characterization and potential applications of NNC 55-0396. *Cardiovasc Drug Rev* **23**:173-196.
- Linden J (1982) Calculating the dissociation constant of an unlabeled compound from the concentration required to displace radiolabel binding by 50%. *J Cyclic Nucleotide Res* **8**:163-172.
- Ma B, Prueksaritanont T and Lin JH (2000) Drug interactions with calcium channel blockers: possible involvement of metabolite-intermediate complexation with CYP3A. *Drug Metab Dispos* **28**:125-130.
- Massie BM (1997) Mibefradil: a selective T-type calcium antagonist. *Am J Cardiol* **80**:231-321.
- Nikonenko I, Bancila M, Bloc A, Muller D and Bijlenga P (2005) Inhibition of T-type calcium channels protects neurons from delayed ischemia-induced damage. *Mol Pharmacol* **68**:84-89.
- Nuss HB and Houser SR (1993) T-type Ca<sup>2+</sup> current is expressed in hypertrophied adult feline left ventricular myocytes. *Circ Res* **73**:777-782.
- Oparil S and Calhoun DA (1991) The calcium antagonists in the 1990s. An overview. *Am J Hypertens* **4**:396S-405S.

DMD #20115

Panner A and Wurster RD (2006) T-type calcium channels and tumor proliferation. *Cell Calcium* **40**:253-259.

Perez-Reyes E, Cribbs LL, Daud A, Lacerda AE, Barclay J, Williamson MP, Fox M, Rees M and Lee JH (1998) Molecular characterization of a neuronal low-voltage-activated T-type calcium channel. *Nature* **391**:896-900.

Portegies MC, Schmitt R, Kraaij CJ, Braat SH, Gassner A, Hagemeyer F, Pozenel H, Prager G, Viersma JW, van der Wall EE and et al. (1991) Lack of negative inotropic effects of the new calcium antagonist Ro 40-5967 in patients with stable angina pectoris. *J Cardiovasc Pharmacol* **18**:746-751.

Prueksaritanont T, Ma B, Tang C, Meng Y, Assang C, Lu P, Reider PJ, Lin JH and Baillie TA (1999) Metabolic interactions between mibefradil and HMG-CoA reductase inhibitors: an in vitro investigation with human liver preparations. *Br J Clin Pharmacol* **47**:291-298.

Rogers R and Prpic R (1998) Profound symptomatic bradycardia associated with combined mibefradil and beta-blocker therapy. *Med J Aust* **169**:425-427.

Russell H. Ellison RP (1997) <http://www.fda.gov/medwatch/SAFETY/1997/posico.htm>.  
*U.S Food and Drug Administration*.

Rutledge A and Triggle DJ (1995) The binding interactions of Ro 40-5967 at the L-type Ca<sup>2+</sup> channel in cardiac tissue. *Eur J Pharmacol* **280**:155-158.

Schmassmann-Suhijar D, Bullingham R, Gasser R, Schmutz J and Haefeli WE (1998) Rhabdomyolysis due to interaction of simvastatin with mibefradil. *Lancet* **351**:1929-1930.

SoRelle R (1998) Withdrawal of Posicor from market. *Circulation* **98**:831-832.

DMD #20115

Stresser DM, Blanchard AP, Turner SD, Erve JC, Dandeneau AA, Miller VP and Crespi

CL (2000) Substrate-dependent modulation of CYP3A4 catalytic activity: analysis of 27 test compounds with four fluorometric substrates. *Drug Metab Dispos* **28**:1440-1448.

Tanaka H and Shigenobu K (2005) Pathophysiological significance of T-type Ca<sup>2+</sup> channels: T-type Ca<sup>2+</sup> channels and drug development. *J Pharmacol Sci* **99**:214-220.

Thummel KE, O'Shea D, Paine MF, Shen DD, Kunze KL, Perkins JD and Wilkinson GR (1996) Oral first-pass elimination of midazolam involves both gastrointestinal and hepatic CYP3A-mediated metabolism. *Clin Pharmacol Ther* **59**:491-502.

Triggle DJ (1991) Sites, mechanisms of action, and differentiation of calcium channel antagonists. *Am J Hypertens* **4**:422S-429S.

Varis T, Backman JT, Kivisto KT and Neuvonen PJ (2000) Diltiazem and mibefradil increase the plasma concentrations and greatly enhance the adrenal-suppressant effect of oral methylprednisolone. *Clin Pharmacol Ther* **67**:215-221.

Venkatakrishnan K, Obach RS and Rostami-Hodjegan A (2007) Mechanism-based inactivation of human cytochrome P450 enzymes: strategies for diagnosis and drug-drug interaction risk assessment. *Xenobiotica* **37**:1225-1256.

Wandel C, Kim RB, Guengerich FP and Wood AJ (2000) Mibefradil is a P-glycoprotein substrate and a potent inhibitor of both P-glycoprotein and CYP3A in vitro. *Drug Metab Dispos* **28**:895-898.

Watanabe A, Nakamura K, Okudaira N, Okazaki O and Sudo K (2007) Risk Assessment for Drug-Drug Interaction Caused by Metabolism-Based Inhibition of CYP3A

DMD #20115

- Using Automated in Vitro Assay Systems and Its Application in the Early Drug Discovery Process. *Drug Metab Dispos* **35**:1232-1238.
- Welker HA and Banken L (1998) Mibefradil pharmacokinetic and pharmacodynamic population analysis. *Int J Clin Pharmacol Res* **18**:63-71.
- Wienkers LC and Heath TG (2005) Predicting in vivo drug interactions from in vitro drug discovery data. *Nat Rev Drug Discov* **4**:825-833.
- Wiltshire HR, Harris SR, Prior KJ, Kozlowski UM and Worth E (1992) Metabolism of calcium antagonist Ro 40-5967: a case history of the use of diode-array u.v. spectroscopy and thermospray-mass spectrometry in the elucidation of a complex metabolic pathway. *Xenobiotica* **22**:837-857.
- Wiltshire HR, Sutton BM, Heeps G, Betty AM, Angus DW, Harris SR, Worth E and Welker HA (1997a) Metabolism of the calcium antagonist, mibefradil (POSICOR, Ro 40-5967). Part III. Comparative pharmacokinetics of mibefradil and its major metabolites in rat, marmoset, cynomolgus monkey and man. *Xenobiotica* **27**:557-571.
- Wiltshire HR, Sutton BM, Heeps G, Betty AM, Angus DW, Madigan MJ and Sharp SR (1997b) Metabolism of the calcium antagonist, mibefradil (POSICOR, Ro 40-5967). Part II. Metabolism in hepatic microsomes from rat, marmoset, cynomolgus monkey, rabbit and man. *Xenobiotica* **27**:539-556.
- Wu S, Zhang M, Vest PA, Bhattacharjee A, Liu L and Li M (2000) A mibefradil metabolite is a potent intracellular blocker of L-type Ca(2+) currents in pancreatic beta-cells. *J Pharmacol Exp Ther* **292**:939-943.

DMD #20115

Yu AM, Idle JR, Krausz KW, Kupfer A and Gonzalez FJ (2003) Contribution of individual cytochrome P450 isozymes to the O-demethylation of the psychotropic beta-carboline alkaloids harmaline and harmine. *J Pharmacol Exp Ther* **305**:315-322.

Zhou S, Yung Chan S, Cher Goh B, Chan E, Duan W, Huang M and McLeod HL (2005) Mechanism-based inhibition of cytochrome P450 3A4 by therapeutic drugs. *Clin Pharmacokinet* **44**:279-304.

DMD #20115

### **Footnotes**

This research is supported by NIEHS grant RO1ES015384 to Oliver Hankinson, by a fellowship to Peter Bui from the University of California Toxic Substances Research and Teaching Program, by the Department of Veterans Affairs, and by the Ralph M. Parsons Foundation.

Correspondence should be addressed to Oliver Hankinson, Ph.D., Departmental of Pathology and Laboratory Medicine, David Geffen School of Medicine, University of California at Los Angeles, 650 Charles Young Drive, Factor 13-244, Los Angeles, CA. 90095, U.S.A,

Tel: +310-825-2936 Fax: +310-794-9272 Email: [ohank@mednet.ucla.edu](mailto:ohank@mednet.ucla.edu)

DMD #20115

## Legends for Figures

Figure 1. Chemical structures of mibefradil, NNC55-0396, and the hydrolyzed metabolite of mibefradil, Ro 40-5966.

Figure 2. Inhibition profile of the activities of various human P450s by 100 nM and 10 $\mu$ M mibefradil (Mib) or NNC55-0396 (NNC). The inhibition activities of (A) CYP1A2, (B) CYP2E1, (C) CYP2C9, (D) CYP2C19, (E) CYP2C8, (F) CYP3A4, and (G) CYP2D6 are expressed relative to the activities of the no inhibitor control (ACN), as the percentage of the inhibited activity over the uninhibited one. Thus, the percent of inhibition is calculated as 100% minus the % listed on the graph. Data are represented as the means  $\pm$  S.D. of duplicate determinations. The \* and \*\*\* indicate  $p < 0.05$  and  $p < 0.001$  for comparison between control (ACN) and inhibitor added samples by an unpaired t-test.

Figure 3. Comparison of mibefradil and NNC55-0936 inhibition of CYP3A4 and CYP2D6. (A) The  $IC_{50}$  and  $K_i$  determination of mibefradil and NNC55 for BFC debenzoylation by CYP3A4. (B) The  $IC_{50}$  and  $K_i$  determination of mibefradil and NNC55-0396 for AMMC N-demethylation by CYP2D6. Data are represented as the averages  $\pm$  S.D. of duplicate determinations. \*\* indicates  $p < 0.005$  comparing the mibefradil and NNC55-0396 samples by a paired t-test.

Figure 4. Inhibition profiles for testosterone and harmaline metabolism in human liver microsomes by mibefradil and NNC55-0936. (A)  $IC_{50}$  and  $K_i$  determination of mibefradil

DMD #20115

and NNC55-0396 for testosterone metabolism mainly by CYP3A in human liver microsomes. \*\*\* indicates  $p < 0.001$  comparing the mibefradil and NNC55-0396 samples by a paired t-test. (B)  $IC_{50}$  and  $K_i$  determination of mibefradil and NNC55-0396 for harmaline metabolism mainly by CYP2D6 in human liver microsomes. \*\* indicates  $p < 0.01$ , for comparing NNC55-0396 to mibefradil by a paired t-test.

Figure 5. Hydrolysis of mibefradil but not NNC55-0396 by pig liver esterase. (A) HPLC chromatograms of 40  $\mu$ M NNC55-0396 incubated with pig liver esterase (solid line), and of a standard for Ro 40-5966 (broken line). The 14 and 15.5 minute peaks correspond to NNC55-0396 and Ro 40-5966, respectively (B) HPLC chromatograms of 40  $\mu$ M mibefradil incubated with pig liver esterase (solid line), and of standard Ro 40-5966 (broken line). The 11.5 and 15.5 minute peaks correspond to mibefradil and Ro 40-5966, respectively. Open arrow indicates the presence of Ro 40-5966 at 15.5 minutes generated by hydrolysis in the mibefradil sample.

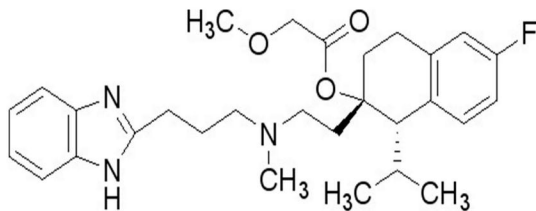
Figure 6. Inhibition profiles of the activities of various human P450s by Ro 40-5966. The  $IC_{50}$  and  $K_i$  determinations of Ro 40-5966 for recombinant (A) CYP2D6, and (B) CYP3A4, and the  $IC_{50}$  determinations for (C) CYP2C9, and (D) CYP1A2. The relative activities of 100 nM and 10  $\mu$ M Ro 40-5966 samples to a control (ACN) catalyzed by recombinant (E) CYP2C19 and (F) CYP2C8.  $IC_{50}$  determinations for CYP2C19 and CYP2C8 were not necessary because they were not strongly inhibited by Ro 40-5966 even at 10  $\mu$ M. Data are represented as the means  $\pm$  S.D. of duplicate determinations. \*

DMD #20115

indicates  $p < 0.05$  comparing control (ACN) and Ro 40-5966 samples by an unpaired t-test.

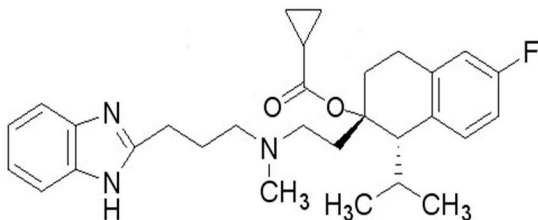
Figure 7. Mechanism-based inactivation of recombinant human CYP3A4 by mibefradil and NNC55-0396. Time and concentration-dependent loss of recombinant CYP3A4 testosterone 6- $\beta$ -hydroxylase activity with mibefradil and NADPH (A) or NNC55-0396 and NADPH (C). The double reciprocal plot of the rates of inactivation as a function of the mibefradil (B) and NNC55-0396 (D) concentration. The values for  $1/K_{obs}$  ( $\text{min}^{-1}$ ) were calculated from the slopes of inactivation experiments by mibefradil or NNC55-0396 in A or C respectively. All the slopes were normalized to the slope of no inhibitor experiment. The  $K_I$  and  $K_{inact}$  values are estimated by 1 divided by the X and Y-intercepts, respectively. \* and \*\* indicate  $p < 0.05$  and 0.01 respectively comparing to control (0 nM) samples by an unpaired t-test.

Figure 1



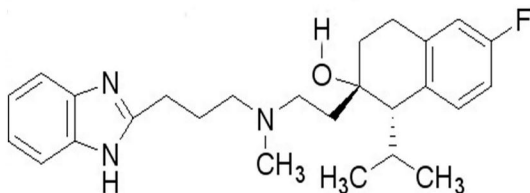
**Mibefradil**,  $C_{29}H_{38}FN_3O_3$

(1S,2S)-2-(2-(N-[(3-Benzimidazol-2-yl)propyl]-N-methylamino)ethyl)-6-fluoro-1,2,3,4-tetrahydro-1-isopropyl-2-naphthyl methoxyacetate dihydrochloride



**NNC-55-0396**,  $C_{30}H_{40}Cl_2FN_3O_2$

(1S,2S)-2-(2-(N-[(3-Benzimidazol-2-yl)propyl]-N-methylamino)ethyl)-6-fluoro-1,2,3,4-tetrahydro-1-isopropyl-2-naphthyl cyclopropanecarboxylate dihydrochloride



**Mibefradil hydrolyzed metabolite, Ro 40-5966**,  $C_{26}H_{33}FN_3O$

(1S,2S)-2-(2-(N-[(3-benzimidazol-2-yl)propyl]-N-methylamino)ethyl)-6-fluoro-1,2,3,4-tetrahydro-1-isopropyl-2-naphthyl hydroxy dihydrochloride

Figure 2

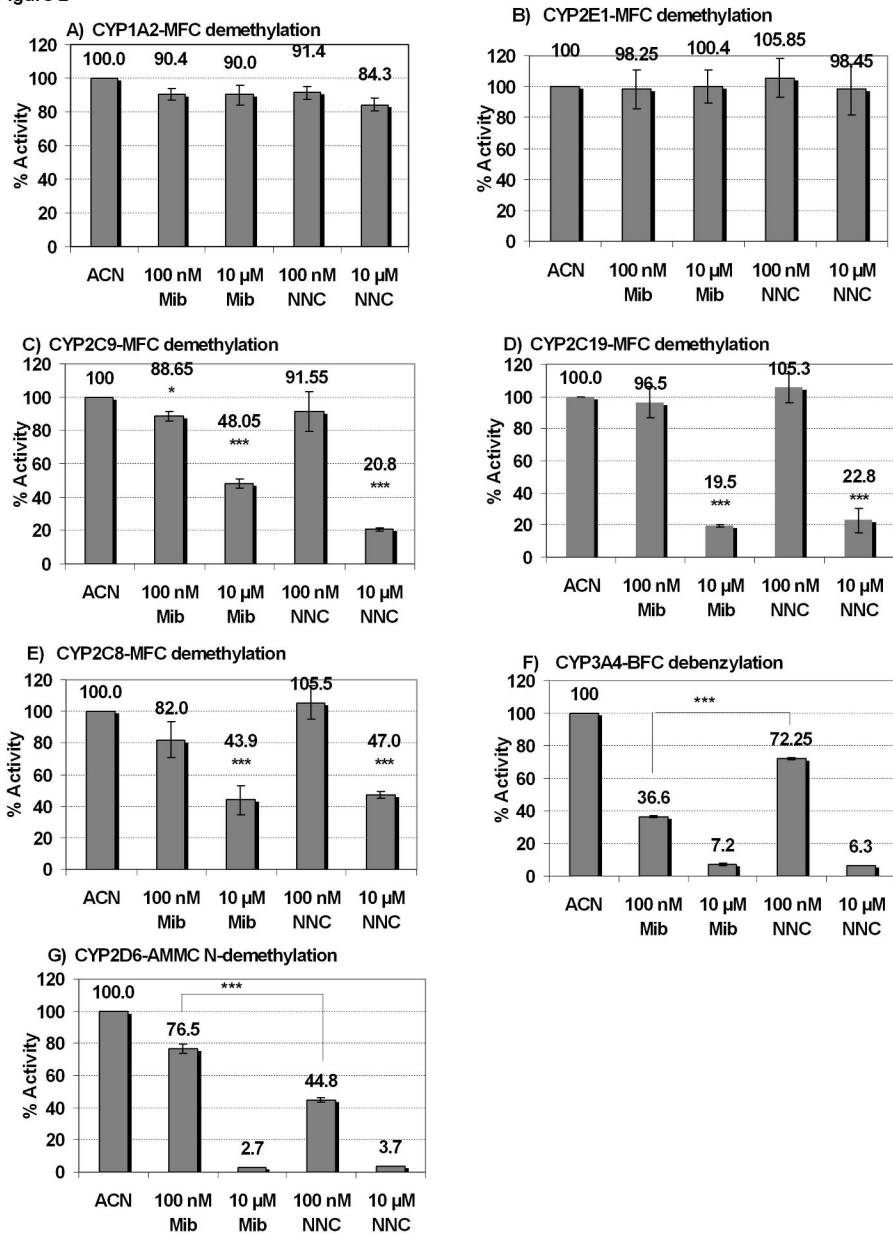
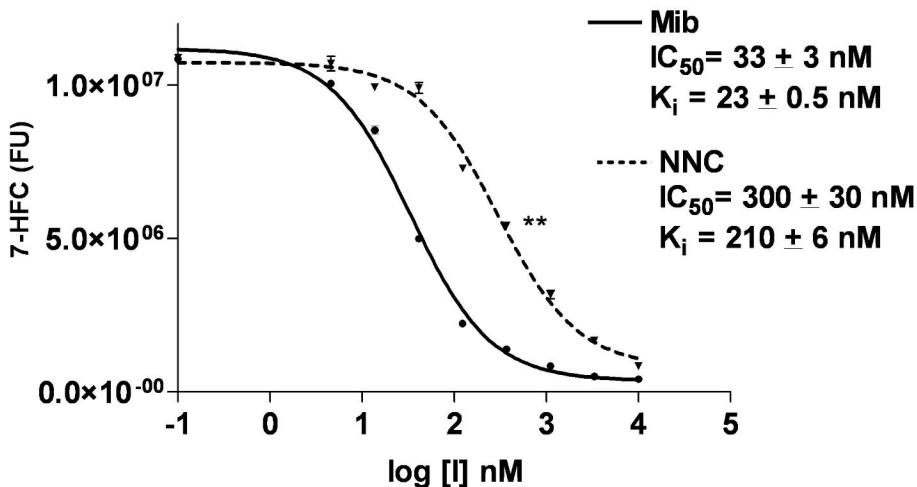


Figure 3

A)  $IC_{50}$  for CYP3A4



B)  $IC_{50}$  for CYP2D6

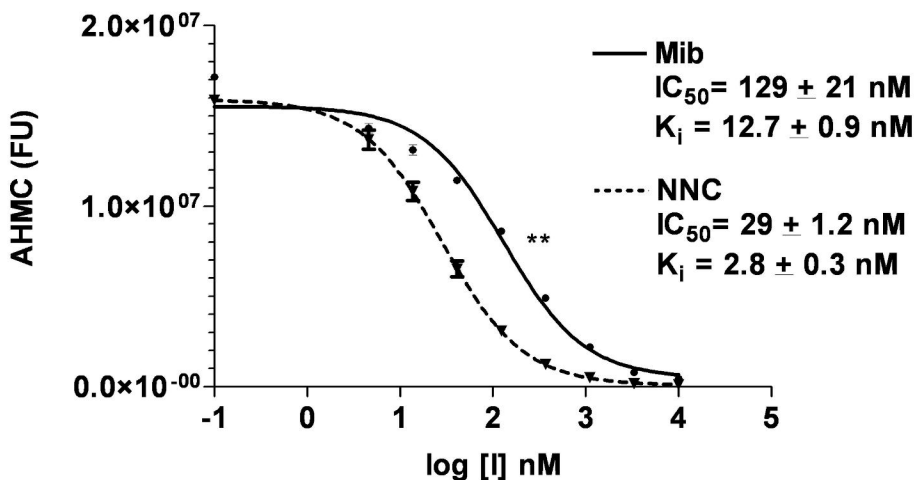
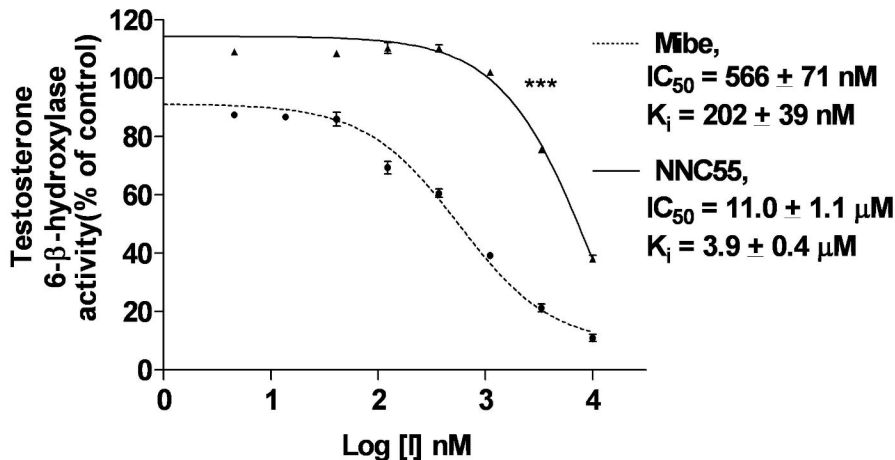


Figure 4

**A) IC<sub>50</sub>-human liver microsomes  
testosterone metabolism**



**B) IC<sub>50</sub>- human liver microsome  
harmaline metabolism**

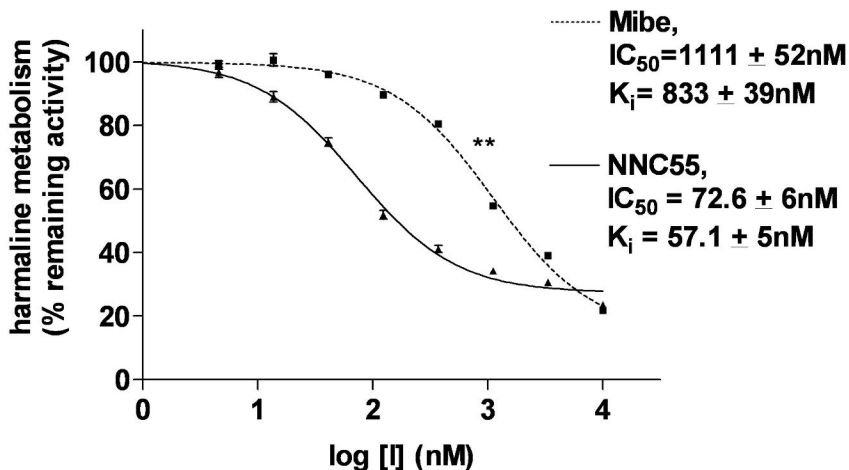


Figure 5

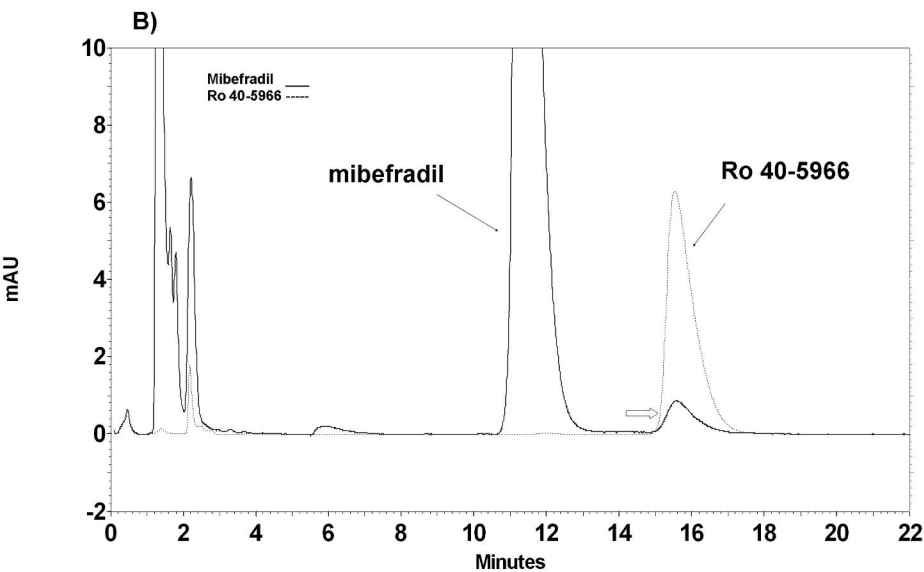
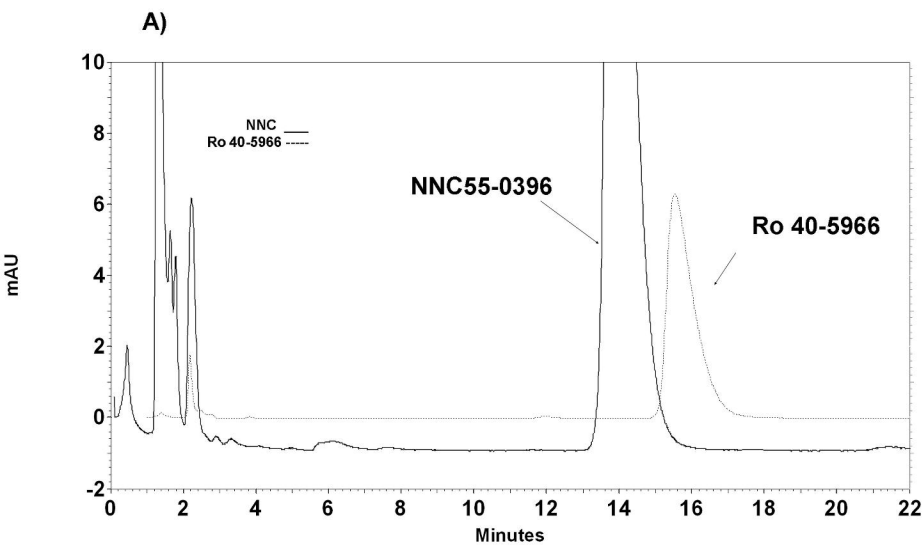
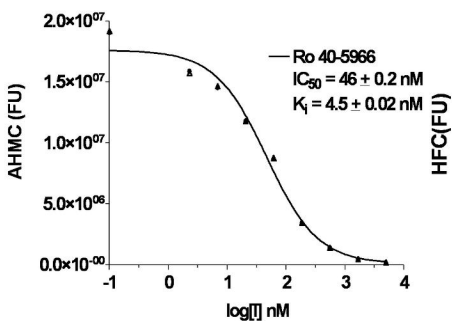
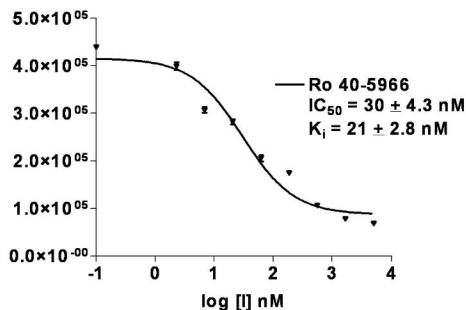


Figure 6

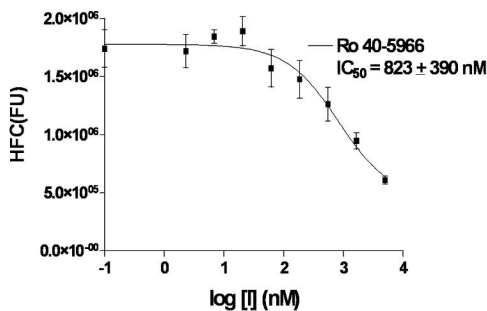
A)  $IC_{50}$  for CYP2D6



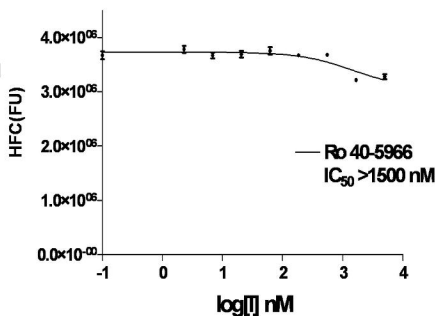
B)  $IC_{50}$  for CYP3A4



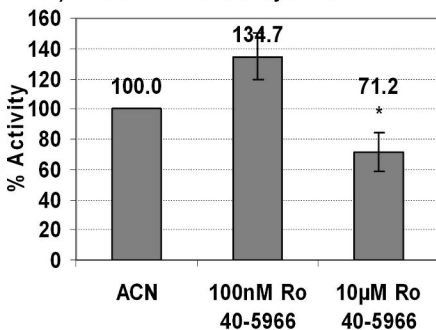
C)  $IC_{50}$  for CYP2C9



D)  $IC_{50}$  for 1A2



E) 2C19-MFC demethylation



F) 2C8-MFC demethylation

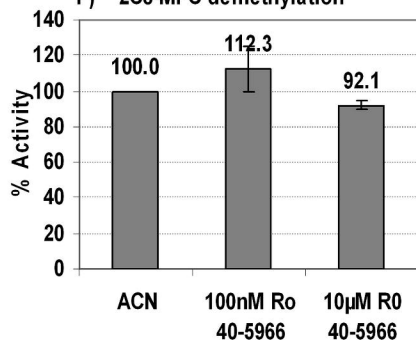
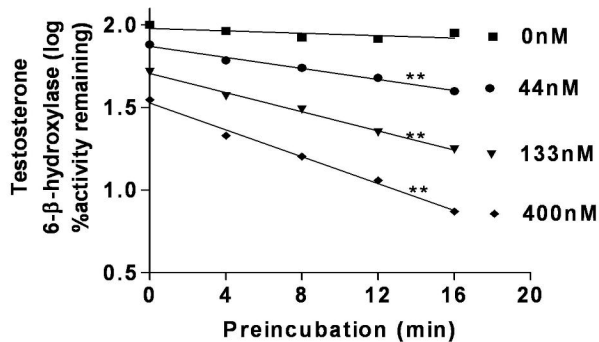
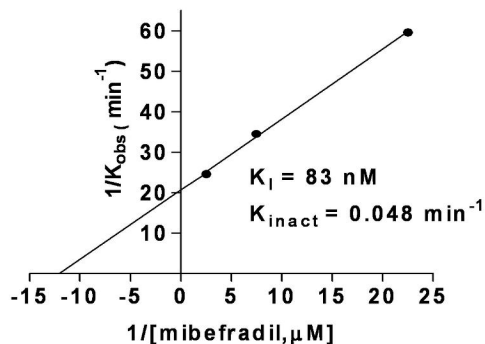


Figure 7

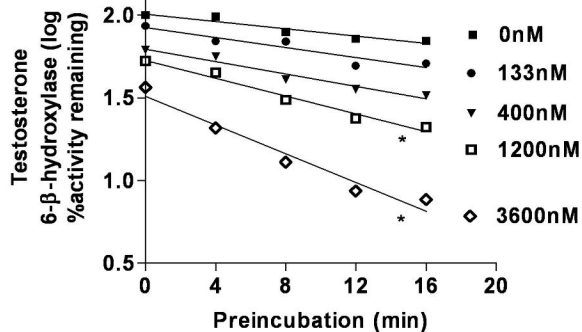
A) Mibefradil-CYP3A4



B) Mibefradil



C) NNC55-0396-CYP3A4



D) NNC55-0396

